

# Coordination of Multiple Renewable Generators Used in a Micro grid Based on Distributed Sub gradient

K.Ramu, A.Tejasri

**Abstract—** Maximum peak power tracking algorithms, which emphasize high renewable energy utilization, may cause a supply-demand imbalance when the available renewable generation is more than demanded, especially for autonomous microgrids. Currently, droop control is one of the most popular decentralized methods for sharing active and reactive loads among the distributed generators. However, conventional droop control methods suffer from slow and oscillating dynamic response and steady state deviations. To overcome these problems, this paper proposes a distributed sub gradient-based solution to coordinate the operations of different types of distributed renewable generators in a microgrid. By controlling the utilization levels of renewable generators, the supply-demand balance can be well maintained and the system dynamic performance can be significantly improved. Simulation results demonstrate the effectiveness of the proposed control solution.

**Index Terms—** Distributed cooperative control, microgrid, multiagent system, renewable generator.

## I. INTRODUCTION

Nearly all energy used was renewable. Almost without a doubt the oldest known use of renewable energy, in the form of traditional biomass to fuel fires, dates from 790,000 years ago. Use of biomass for fire did not become commonplace until many hundreds of thousands of years later, sometime between 200,000 and 400,000 years ago. Probably the second oldest usage of renewable energy is harnessing the wind in order to drive ships over water. This practice can be traced back some 7000 years, to ships on the Nile. Moving into the time of recorded history, the primary sources of traditional renewable energy were human labor, animal power, water power, wind, in grain crushing windmills, and firewood, a traditional biomass. A graph of energy use in the United States up until 1900 shows oil and natural gas with about the same importance in 1900 as wind and solar played in 2010. By 1873, concerns of running out of coal prompted experiments with using solar energy. Development of solar engines continued until the outbreak of World War I. The importance of solar energy was recognized in a 1911 Scientific American article: "in the far distant future, natural fuels having been exhausted [solar power] will remain as the only means of existence of the human race".

The theory of peak oil was published in 1956. In the 1970s environmentalists promoted the development of renewable energy both as a replacement for the eventual depletion of oil,

as well as for an escape from dependence on oil, and the first electricity generating wind turbines appeared. Solar had long been used for heating and cooling, but solar panels were too costly to build solar farms until 1980. An autonomous microgrid, the control issues are very similar to those of large-scale power systems, such as supply-demand balance and frequency regulation. Due to the similarity, most existing ideas on traditional power system operation can be introduced to small scale autonomous microgrids. In [6], the authors propose a two-level control scheme for a wind farm, which consists of supervisory and machine levels of control. In this scheme, the supervisory control level decides the active and reactive power set points for all doubly-fed induction generators (DFIGs), while the machine control level ensures that the set points are reached. In [7], the authors propose an optimal dispatch control strategy for a wind farm. The DFIGs were controlled to adjust the active and reactive power generation according to the request of the system's central operator. In [8], the authors present a control approach for a wind farm to provide a sufficient generating margin upon the request of supervisory controllers. In [9], the authors present a coordinated control method for leveling photovoltaic (PV) generation. This control scheme uses fuzzy reasoning to generate the central leveling generation commands to reduce the frequency deviation of the isolated power utility.

All of these methods are centralized, therefore requiring complicated communication networks to collect information globally [10] and a powerful central controller to process huge amounts of data. Thus, these solutions are costly to implement and susceptible to single-point failures. Due to the intermittency of renewable generation, more frequent control updates are required. The centralized solutions may not be able to respond in a timely fashion if operating conditions change rapidly and unexpectedly. This paper targets small-scale, self-contained, medium voltage microgrid power systems, which are composed of multiple RGs, a reliable synchronous generator (SG), and loads. For a microgrid to work autonomously, it must maintain its own supply-demand balance in terms of active power and regulate the system frequency and voltage magnitudes.

## II. PROPOSED SUBGRADIENT-BASED SOLUTION

This section introduces the proposed fully-distributed algorithm, which can achieve the system's power supply-demand balance within the microgrid.

### A. Utilization Level Based Coordination

The total active power demand ( $P_D$ ) of a microgrid can be calculated as

$$P_D = \sum_{i=1}^n P_{L,i} + P_{Loss}$$

$$u^* = \min \left\{ \frac{P_D}{P_G^{\max}}, 1 \right\}$$

Where  $n$  is the number of buses in the microgrid,  $P_{L,i}$  is the demand of load at bus  $i$ , and  $P_{Loss}$  is the active power loss in the microgrid.

The total available renewable power generation in the microgrid can be calculated as

$$P_{G,i}^{ref} = u^* \cdot P_{G,i}^{\max} \quad (3)$$

where  $n$  is the number of RGs, and  $P_{G,i}^{\max}$  is the maximum power generation of RG  $i$ . In an autonomous microgrid, if  $P_G^{\max}$  is less than  $P_D$ , all RGs will operate in MPPT mode, and the SG(s) should compensate the generation deficiency. On the other hand, if  $P_G^{\max}$  is larger than  $P_D$ , MPPT control strategies no longer apply. A suitable deloading strategy is required to share the load demands among the RGs, which can be accomplished by controlling the utilization levels ( $u_i$ ,  $s$ ) of RGs to a common value.

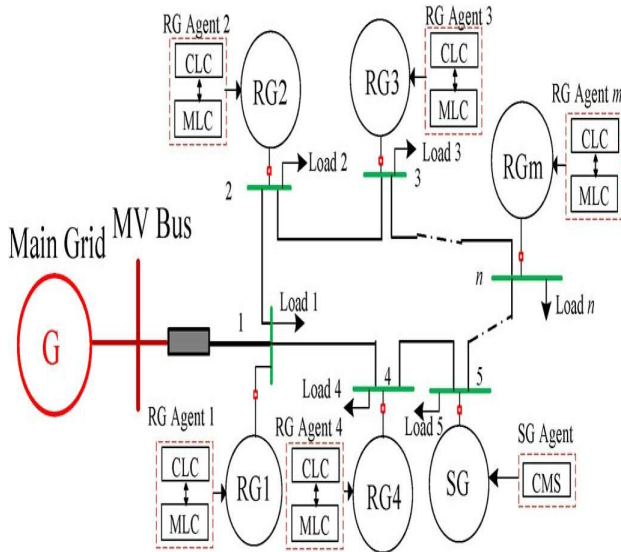


Fig. 1. Illustration of the control topology of a microgrid.

### B. Algorithm Implementation

The proposed control topology is shown in Fig. 1, which is mainly composed of RGs, an SG and loads. Each RG is assigned an RG agent. An RG agent can measure the system's frequency, predict its maximum renewable power generation, and exchange information with its neighboring agents. The supporting communication system for the MAS based solutions can be designed to be independent to the topology of the power network. Even for a complex system, simple communication network can be designed base on cost, location, convenience, etc. Each SG is assigned an SG agent, which does not participate in the utilization level updating process. The SG agent decides the control mode of the SG through control mode selection (CMS),

According to the proposed distributed algorithm, there is no need to measure global loading conditions and losses in the system. Since any supply demand imbalance will result in changes in frequency, the utilization level of an RG can be

adjusted based on measured frequency deviation as shown in (23). In this way, the amount of measurements can be significantly reduced. In addition, the complexity and cost of the supporting communication network can also be lowered. The maximum active power generation of a DFIG can be estimated using measured wind speed [37]. In addition, there are many other MPPT algorithms for wind turbine generators available in literature, as summarized in [38]. Similarly, the maximum generation of a PV generator can be predicted based on weather condition (solar insolation, temperature, etc.) [39].

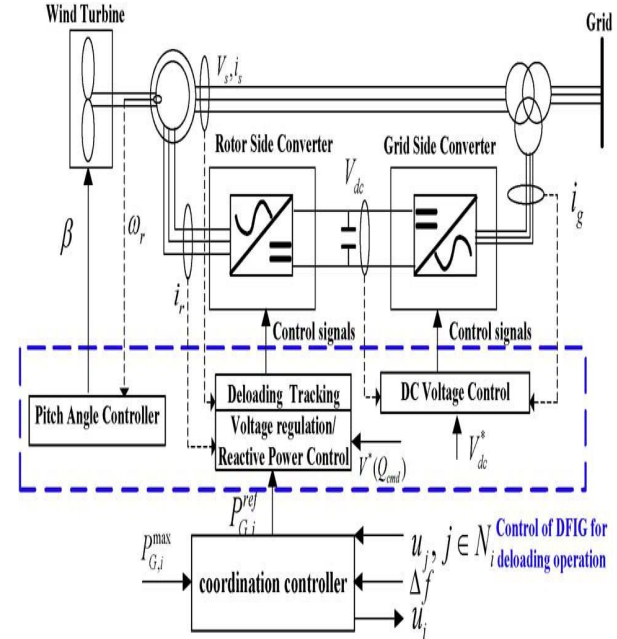


Fig.2. Machine-level control of DFIG in deloading mode.

A lot of MPPT algorithms for PV generators have been developed in the past years [40], such as, fuzzy logic control, neural network, etc. In accuracy of the maximum power estimation always exists to some extent due to the prediction errors [41]. Sometimes the predicted value is larger than practical, sometimes smaller. For under-estimation, the predicted generation can be realized. For over-estimation, such as due to the aging problem or internal failures of a PV system, the advantage of the proposed algorithm will present. The proposed algorithm updates generation references based on overall generation estimations and overall demand. Since the generation reference settings are usually lower than the  $P_{G,i}^{\max}$  under sufficient renewable generation, the impact of inaccurate estimation can be lowered.

### III. SIMULATION STUDIES

The proposed fully-distributed cooperative control algorithm is tested with a 6-bus microgrid model using MATLAB/SIMULINK. In this paper, the DFIG is controlled by back-to-back converters. With the decoupled control method introduced in [43], the rotor-side converter (RSC) controls both the active and reactive power of the DFIG. The active power is controlled by adjusting the  $d$ -axis rotor current, while the reactive power is controlled by adjusting the  $q$ -axis rotor current, as shown in Fig.3.

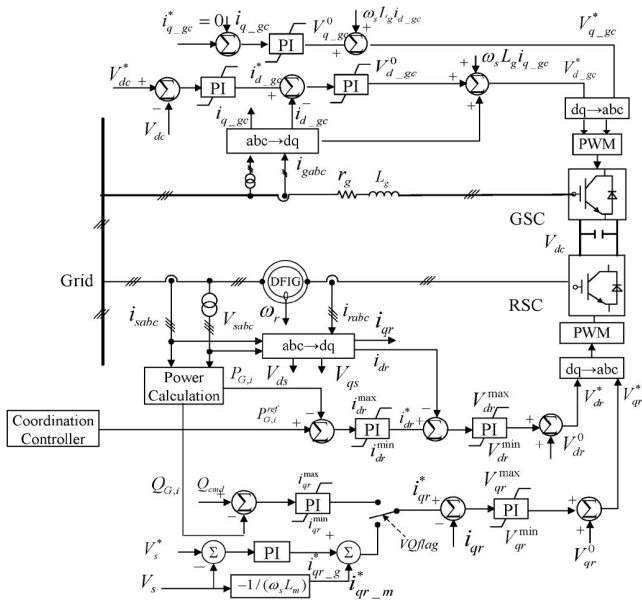


Fig.3. Schematic diagram of control strategy for RSC and GSC of a DFIG.

The deviation between the active power output of DFIG and the reference value forms the error signal that is processed by a PI controller to produce the rotor current reference. Through another PI controller, the difference between rotor current and reference value is used to produce rotor voltage. There are two modes for reactive power control, the voltage and reactive power regulation modes. Both modes regulate q-axis rotor current. In voltage regulation mode, is controlled to reduce voltage fluctuation [44]. For reactive power regulation, the difference between the reactive command and the reactive power output forms rotor current reference through a PI controller. Here, GSC is used only to stabilize the DC-link voltage.

as shown in Fig.4. The system contains six loads, three DFIGs, two PVs and one SG. The DFIG at bus-1 (abbreviated as DFIG-1) is controlled in reactive power regulation mode, the DFIG-4 and DFIG-5 are controlled

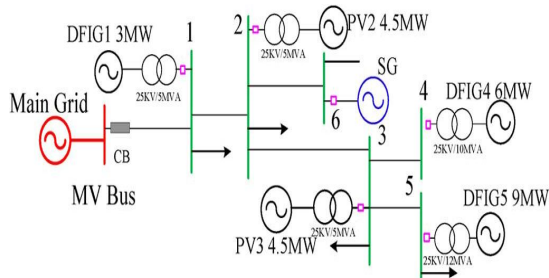


Fig.4. Configuration of a 6-bus microgrid.

in voltage regulation mode, and the PV-2 and PV-3 are controlled in unit power factor mode, as introduced in Section III. The ramp-up and ramp-down rates of the SG are both set to 0.4 MW/s. The communication topology of the MAS for the 6-bus microgrid. During simulations, time step for utilization level update is selected to be 0.1 s, which has good balance of control performance and technical feasibility. The proposed control strategy is tested under two operating conditions. Test 1 establishes a constant available renewable generation and loads. Test 2 has variable available

renewable generation and loads. The first test is unrealistic yet easier to understand due to its simplicity.

### A. Test 1

In the first test, the demands of the loads remain constant. The wind speeds of the DFIGs at bus-1, bus-4, and bus-5 are constant at 11 m/s, 14 m/s, and 14 m/s, respectively. The solar insolation of PVs at bus-2 and bus-3 are 900W/m<sup>2</sup> and 1000W/m<sup>2</sup>, respectively. An islanding event at 20 s is simulated to test the performance of the proposed control strategy. Before islanding, RGs are controlled using the MPPT algorithm, and the initial output of the SG is set to 2 MW to create enough disturbances to test the performance of the proposed control algorithm. At the instant of islanding, the available renewable power is more than the load demand, the system's frequency increases at this moment. The proposed algorithm forces the utilization level to drop in order to allow the RGs to dump excessive renewable power. Fig.5 shows the dynamic responses of the RGs. The active power generations of the DGs converge to a value below the maximum available power after islanding. The utilization levels, if calculated, are the same as the ratio of actual output power to MPPT power. To evaluate the performance of the proposed algorithm, the traditional Droop-AGC method is simulated for comparison. Droop control is used to adjust the generations based on predefined P-f-Q-V characteristic. AGC is applied every 5 s to eliminate frequency deviation. The dynamic responses under the proposed algorithm and Droop-AGC method are shown in Figs.6

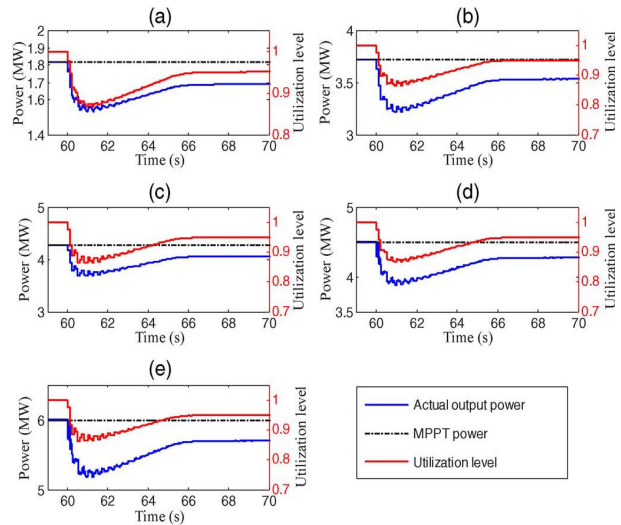


Fig.5. Dynamic response of DGs. (a) DFIG-1 active power output; (b) PV-2 active power output; (c) PV-3 active power output; (d) DFIG-4 active power output; (e) DFIG-5 active power output.

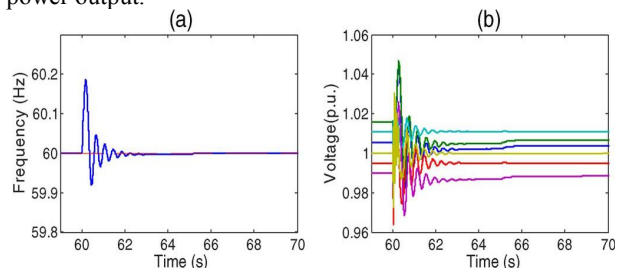


Fig.6. System response under the proposed solution. (a) Frequency response; (b) terminal voltages of DGs.



and 7, respectively. By comparing Figs. 6(a) and 7(a), one can see that the frequency response under the proposed solution is able to converge to the nominal value within 6 s, while it takes the Droop-AGC method 30 s to converge. In addition, the overshoot of frequency response under the proposed algorithm is 0.19 Hz, which is much smaller than that of the conventional droop method(0.32 Hz). Similar observations can be made for voltage responses under the proposed algorithm and Droop-AGC method, as shown in Figs.6(b) and 7(b), respectively.

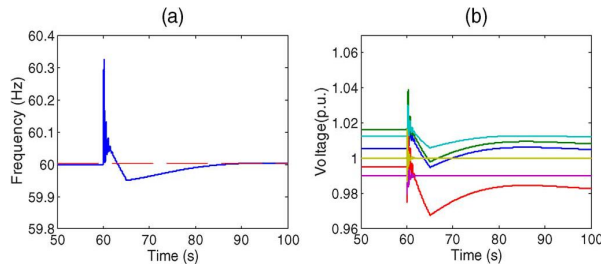


Fig.7. System response under the Droop-AGC method. (a) Frequency response; (b) terminal voltages of DGs.

The improved performance comes from dynamic and accurate generation adjustments as compared to using fixed P-f and Q-V characteristics.

**B. Test 2**

In this test, the initial output of the SG is intentionally set to 4MW. The sequence of events in this simulation consists of the microgrid being isolated from the main grid at 60 s, and then a load of 2 MW being shed at 150 s and restored at 200 s.the proposed algorithm is good at coordinating the utilization level of five RGs to a common value. The utilization level drops below 1 immediately after grid disconnection. The SG switches to voltage regulation mode and its active power generation gradually decreases from 4MW to zero.It Utilizationes level profiles of 5 RGs (Test 2).according to the pre-defined ramp-down rate. At 150 s, a load of 2 MW is shed, and the utilization level drops so that the RGs can reduce the renewable generation. The utilization level rises at 200 s when the load is restored. When the estimated maximum renewable generation is insufficient, the utilization level reaches the upper bound and is capped at 1, and all of the RGs are controlled in MPPT mode, which can be observed during the period from 228 s to 300s. When the loads are modeled as serial RLC modules with constant parameters, the actual load will oscillate due to frequency and voltage fluctuations. Investigating the responses of the frequency and terminal voltages (Fig.8)

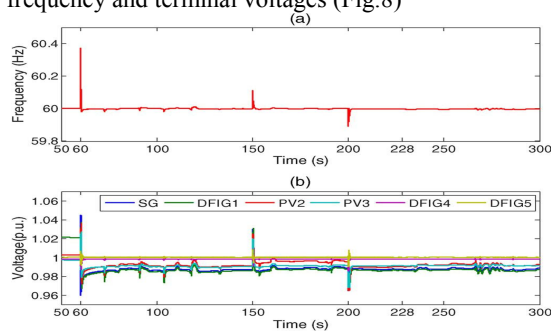


Fig.8. System response of test 2. (a) System frequency response; (b) terminal voltages of DGs.

helps to clarify this phenomenon.the utilization level, the actual active power generation, and the available maximum wind power of DFIG-4. DFIG-4 can operate in deloading mode when the available renewable power exceeds the demand (60 s–228 s) and in MPPT mode when the available maximum renewable power is insufficient (228 s–300 s). Similar performances can be observed for other RGs, which are not shown here. When the rotor speed is below the threshold of 1.3 p.u., the pitch angle control is not activated and remains at .Pitch angle control is activated when the rotor speed reaches the upper limit. The frequency and voltage responses are usually customers’ main concerns, and they should be evaluated by up-to-date standards and regulation codes. According to the IEEE Std. 1547 [53], the normal frequency should be within the range of 59.8 Hz–60.5 Hz. ANSI/NEMA C84.1 [54] recommends that the frequency deviation should be within 0.05 Hz and the voltage within 0.90 p.u.–1.10 p.u. Fig.8 indicates that the maximum frequency deviation (60.4 Hz) is less than 60.5 Hz, and the voltage response is in the range of (0.96 p.u.–1.05p.u.).Therefore, both the frequency and voltage performances meet the above standards. During the simulation study, DFIG-4 and DFIG-5 are operated in voltage regulation mode, and the SG, DFIG-1, PV-2 and PV-3 are operated in reactive power generation mode. In the latter mode, a fixed amount of reactive power is generated, and there is no direct control of the terminal voltage. This is why the terminal voltage responses of buses in voltage regulation mode are much better than those of the other buses.

CONCLUSION

This paper targets at the coordination problem with an autonomous microgrid under high penetration of renewable energy. Two main reasons motivate the authors to control the utilization level to a common value instead of controlling some RGs in MPPT mode and others in reduced generation mode. First, MPPT algorithms that emphasize high renewable energy utilization may cause supply-demand imbalance when the available renewable generation is more than demanded. Second, every MPPT algorithm has the problem of impreciseness to certain degree and the predicted maximum available generation might be unachievable. By synchronizing the utilization levels of the RGs to a common value, the impacts of prediction impreciseness of the MPPT algorithms can be efficiently mitigated.The proposed control scheme has the following four main advantages. The first advantage is the introduction of a simple MAS-based fully distributed method. Due to the simplicity of the network topology and the reduced amount of information to exchange, the cost of the supporting communication network will be much lower than that of a centralized solution. The second is its avoidance of the direct measurements of loading conditions. The third is its distributed coordination of different types of DGs (DFIG, PV, and SG), which can maintain the supply-demand balance within the microgrid. The fourth is its introduction of the subgradient optimization method, which improves the system’s dynamic performance. Simulation studies demonstrate that the multiple RGs and the SG are well coordinated to maintain the power supply-demand balance for the autonomous microgrid in both excessive and insufficient available renewable power situations.

REFERENCES

- [1] S. Abu-Sharkh, R. J. Arnold, J. Kohler, and R. Li, "Can microgrids make a major contribution to UK energy supply?," *Renew. Sustain. Energy Rev.*, vol. 10, no. 2, pp. 78–127, 2006.
- [2] A. Mehrizi-Sani, A. H. Etemadi, D. E. Olivares, and R. Iravani, "Trends in microgrid control," *IEEE Trans. Smart Grid*, to be published.
- [3] N. Femia, G. Petrone, G. Spagnuolo, and M. Vitelli, "Optimization of perturb and observe maximum power point tracking method," *IEEE Trans. Power Electron.*, vol. 20, no. 4, pp. 963–973, 2005.
- [4] E. Koutroulis and K. Kalaitzakis, "Design of a maximum power tracking system for wind-energy-conversion applications," *IEEE Trans. Ind. Electron.*, vol. 53, no. 2, pp. 486–494, 2006.
- [5] L. Qu and W. Qiao, "Constant power control of DFIG wind turbines with supercapacitor energy storage," *IEEE Trans. Ind. Applicat.*, vol. 47, no. 1, pp. 359–367, 2011.
- [6] J. L. Rodriguez-Amenedo, S. Arnalte, and J. C. Burgos, "Automatic generation control of a wind farm with variable speed wind turbines," *IEEE Trans. Energy Convers.*, vol. 17, no. 2, pp. 279–284, 2002.
- [7] R. G. de Almeida, E. D. Castronuovo, and J. A. P. Lopes, "Optimum generation control in wind parks when carrying out system operator requests," *IEEE Trans. Power Syst.*, vol. 21, no. 2, pp. 718–725, May 2006.
- [8] L. R. Chang-Chien, C. M. Hung, and Y. C. Yin, "Dynamic reserve allocation for system contingency by DFIG wind farms," *IEEE Trans. Power Syst.*, vol. 23, no. 2, pp. 729–736, May 2008.
- [9] T. Senjyu, A. Yona, M. Datta, H. Sekine, and T. Funabashi, "A coordinated control method for leveling output power fluctuations of multiple PV systems," in *Proc. Int. Conf. Power Electronics*, 2007, pp. 445–450.
- [10] H. Xin, Z. Qu, J. Seuss, and A. Maknouninejad, "A self-organizing strategy for power flow control of photovoltaic generators in a distribution network," *IEEE Trans. Power Syst.*, vol. 26, no. 3, pp. 1462–1473, Aug. 2011.
- [11] A. Dimeas and N. Hatzigiorgiou, "A multiagent system for microgrids," in *Proc. IEEE Power Engineering Society General Meeting*, 2004, vol. 1, pp. 55–58.
- [12] C. M. Colson and M. H. Nehrir, "Algorithms for distributed decisionmaking for multi-agent microgrid power management," in *Proc. 2011 IEEE Power and Energy Society General Meeting*, 2011, pp. 1–8.
- [13] B. Zhao, C. X. Guo, and Y. J. Cao, "A multiagent-based particle swarm optimization approach for optimal reactive power dispatch," *IEEE Trans. Power Syst.*, vol. 20, no. 2, pp. 1070–1078, May 2005.
- [14] A. L. Kulasekera, R. A. R. C. Gopura, K. T. M. U. Hemapala, and N. Perera, "A review on multi-agent systems in microgrid applications," in *Proc. 2011 IEEE PES Innovative Smart Grid Technologies*, 2011, pp. 173–177.
- [15] Y. Xu and W. Liu, "Novel multi agent based load restoration algorithm for microgrids," *IEEE Trans. Smart Grid*, vol. 2, no. 1, pp. 140–149, 2011.
- [16] Y. Xu, W. Liu, and J. Gong, "Multi-agent based load shedding algorithm for power systems," *IEEE Trans. Power Syst.*, vol. 26, no. 4, pp. 2006–2014, Nov. 2011.
- [17] W. Zhang, Y. Xu, W. Liu, F. Ferrese, and L. Liu, "Fully distributed coordination of multiple DFIGs in a microgrid for load sharing," *IEEE Trans. Smart Grid*, to be published.
- [18] F. Ferrese et al., "Cooperative federated control with application to tracking control," in *Proc. 2011 IEEE 13th Int. Conf. High Performance Computing and Communications (HPCC)*, 2011.
- [19] Q. Dong, K. Bradshaw, F. Ferrese, L. Bai, and S. Biswas, "Cooperative federated multi-agent control of large-scale systems," *Control Applicat.*, 2011.
- [20] S. Biswas, F. Ferrese, Q. Dong, and L. Bai, "Resilient consensus control for linear systems in a noisy environment," in *Proc. IEEE American Control Conf. (ACC)*, 2012, Jun. 2012, pp. 5862–5867.
- [21] L. Xiao and S. Boyd, "Optimal scaling of a gradient method for distributed resource allocation," *J. Optimiz. Theory Applicat.*, vol. 29, no. 3, pp. 469–488, 2006.
- [22] A. Nedic and A. Ozdaglar, "Distributed subgradient methods for multiagent optimization," *IEEE Trans. Autom. Control*, vol. 54, no. 1, pp. 48–61, 2009.
- [23] I. Lobel and A. Ozdaglar, "Distributed subgradient methods for convex optimization over random networks," *IEEE Trans. Autom. Control*, vol. 56, no. 6, pp. 1291–1306, 2011.
- [24] J. W. O'Sullivan and M. J. O'Malley, "Identification and validation of dynamic global load model parameters for use in power system frequency simulations," *IEEE Trans. Power Syst.*, vol. 11, no. 2, pp. 851–857, May 1996.
- [25] M. C. Chandorkar and D. M. Divan, "Control of parallel connected inverters in standalone AC supply system," *IEEE Trans. Ind. Applicat.*, vol. 29, no. 1, pp. 136–143, 1993.
- [26] S. J. Chiang and J. M. Chang, "Parallel control of the UPS inverters with frequency-dependent droop scheme," in *Proc. 2001 IEEE 32<sup>nd</sup> Annual Power Electronics Specialists Conf.*, 2001, vol. 2, pp. 957–961.